

# Mapping spatial persistent large deviations of nonequilibrium surface growth processes onto the temporal persistent large deviations of stochastic random walk processes

M. Constantin<sup>1,2</sup> and S. Das Sarma<sup>1</sup><sup>1</sup>*Condensed Matter Theory Center, Department of Physics, University of Maryland, College Park, Maryland 20742-4111, USA*<sup>2</sup>*Materials Research Science and Engineering Center, Department of Physics, University of Maryland, College Park, Maryland 20742-4111, USA*

(Received 29 March 2004; revised manuscript received 18 June 2004; published 29 October 2004)

Spatial persistent large deviations probability of surface growth processes governed by the Edwards-Wilkinson dynamics,  $P_x(x,s)$ , with  $-1 \leq s \leq 1$  is mapped isomorphically onto the temporal persistent large deviations probability  $P_t(t,s)$  associated with the stochastic Markovian random walk problem. We show using numerical simulations that the infinite family of spatial persistent large deviations exponents  $\theta_x(s)$  characterizing the power-law decay of  $P_x(x,s)$  agrees, as predicted on theoretical grounds by Majumdar and Bray [Phys. Rev. Lett. **86**, 3700 (2001)], with the numerical measurements of  $\theta_t(s)$ , the continuous family of exponents characterizing the long-time power law behavior of  $P_t(t,s)$ . We also discuss the simulations of the spatial persistence probability corresponding to a discrete model in the Mullins-Herring universality class, where our discrete simulations do not agree well with the theoretical predictions perhaps because of the severe finite-size corrections which are known to strongly inhibit the manifestation of the asymptotic continuum behavior in discrete models involving large values of the dynamical exponent and the associated extremely slow convergence to the asymptotic regime.

DOI: 10.1103/PhysRevE.70.041602

PACS number(s): 68.37.Ef, 68.35.Ja, 05.20.-y, 05.40.-a

Non-Markovian Gaussian stochastic processes are very widely encountered in a large variety of nonequilibrium physical problems [1]. Considerable theoretical [2] and experimental [3–6] efforts have recently been devoted to understanding the first-passage statistics in such nonequilibrium systems. Recent work [7] has revealed that the time-dependent history of the non-Markovian processes can be described by a nontrivial exponent,  $\theta_r$ , called the persistence exponent, which depends on the dimensionality of the problem,  $d$ , and the precise details of the non-Markovian nature of the underlying stochastic dynamics characterizing the phenomenon. The persistence exponent  $\theta_t$  describes the asymptotic power-law decay of the persistence probability [ $P_t(t) \propto t^{-\theta_t}$ ] which measures the probability that a stochastic variable has not changed its characteristics up to time  $t$ . As a consequence,  $\theta_t$  provides useful quantitative predictions concerning the temporal evolution characteristics of a given stochastic system. Once the persistence probability behavior is found, one can immediately calculate the asymptotic behavior of the first-passage probability,  $F(t)$ , which represents the distribution of the time when the stochastic variable under consideration *first* reaches a fixed reference value:  $F(t) = -dP_t(t)/dt$ . In addition, one can also obtain the mean first-passage time which provides the representative time scale characterizing the stability of the dynamical process. Such a time scale might be of interest for the study of the evolution of fluctuating interfaces or for understanding the behavior of a collection of stochastic spin variables. To be specific, we mention that  $P_t(t)$  and  $\theta_t$  are the *temporal* persistence probability and exponent, respectively, since we also discuss *spatial* persistence  $P_x(x)$  and the corresponding exponent  $\theta_x$ .

Of particular interest in the field of surface growth phenomena is the role played by the dynamics of interfaces which are governed by thermal fluctuations. An illustrative

category of such interfaces is described by linear Langevin equations of the type

$$\partial h(x,t)/\partial t = -(-\nabla^2)^{z/2}h(x,t) + \xi(x,t), \quad (1)$$

where  $h(x,t)$  is the step height fluctuation corresponding to the lateral step position  $x$ , at time  $t$ ,  $\xi(x,t)$  is a white uncorrelated Gaussian noise, and  $z$  is the dynamical exponent. It turns out that fluctuating interfaces are of crucial importance at very small scales (i.e., nanoscales) involved in the fabrication of current electronic devices. In addition to the traditional way of analyzing various aspects of growth processes based on the dynamical scaling behavior of the interface width and temporal and spatial correlation functions [8,9], it has been shown that persistence properties provide an additional tool of investigation for understanding the long time evolution of surface growth phenomena, due to the ability of the nontrivial persistence exponents to identify the underlying universality class of the dynamical process [10] and the presence of the nonlinearities associated with the dynamical evolution [11]. However, much broader and more general information can be extracted from the natural generalization of the persistence through the probability of persistent large deviations [12],  $P_t(t,s)$ , where  $-1 \leq s \leq 1$ . A closely related concept, the sign-time distribution, has been introduced in Ref. [13].  $P_t(t,s)$  measures the probability that the average sign,  $S_{av}(t) = (1/t) \int_0^t \text{sgn}[h(x,t_0+t') - h(x,t_0)] dt'$ , remains always above a particular value  $s$  up to time  $t$  measured from the initial time  $t_0$ . It turns out that  $P_t(t,s)$  provides an infinite family of temporal persistence exponents,  $\theta_t(s)$ , associated with the power-law decay of  $P_t(t,s)$  observed to exist at large time scales for systems belonging to different universality classes [14] relevant for surface growth. In the limit  $s \rightarrow 1$ , the exponent of persistent large deviations reaches the

value of the nontrivial persistence exponent, i.e.,  $\theta_l(s=1) = \theta_l$ . We note that the concept of persistent large deviations naturally generalizes the concept of persistence exponent from a single discrete exponent  $\theta_l$  characterizing the universality class to a more general and deeper concept of a continuous function,  $\theta_l(s)$ , of the persistent exponents characterizing the stochastic dynamics.

The dynamics of the spatially extended systems with fluctuations governed by stochastic differential equations can be further elucidated by looking, in addition to the statistical tools mentioned above, at the *spatial* analog of the temporal persistence, i.e., the spatial persistence probability [15,16],  $P_x(x)$ , and its associated exponents.  $P_x(x)$  represents the probability that the height stochastic variable, measured at a fixed time  $t$ , does not reach its initial value  $h(x_0, t)$  up to a longer distance  $x$  measured from the initial position  $x_0$ . Theoretical [15] and numerical studies [16] indicate that the power-law decay of  $P_x(x)$  is described by two different exponents, the steady-state ( $\theta_{SS}$ ) and the finite initial conditions ( $\theta_{FIC}$ ) spatial persistence exponents depending on the selection rules applied to  $x_0$ : (i)  $\theta_{SS}$  is obtained if  $x_0$  is sampled from the entire set of the steady-state configurational sites, and (ii)  $\theta_{FIC}$  is obtained if  $x_0$  is sampled from a subset of the steady-state sites characterized by *finite* height and height derivatives. The aim of this paper is to establish numerically the concept of *spatial* persistent large deviations probability,  $P_x(x, s)$  with  $-1 \leq s \leq 1$ , as a natural generalization of the spatial persistence probability concept. We also show that  $P_x(x, s)$  measured for growth processes in the well-studied Edwards-Wilkinson [17] universality class [described by Eq. (1) with  $z=2$ ] can be mapped isomorphically onto  $P_l(t, s)$  of the simple random walk stochastic problem. This mapping possibility is inspired by the work of Majumdar and Bray [15], who have shown in a recent Letter that the *spatial* persistence probability characteristics of growth processes involving the interfacial height stochastic variable  $h(x, t)$  with the dynamics described by Eq. (1) can be mapped onto the *temporal* persistence characteristics of the ‘‘random walk’’ processes of the type  $d^n x/dt^n = \eta(t)$ , where  $n=(z-d+1)/2$  and  $\eta(t)$  is a white noise as well. The purpose of the current paper is to show that this exact mapping, as expected, works for the generalized (large deviations) persistence probability and the corresponding continuous family of persistence exponents as well, and to numerically calculate  $\theta_x(s)$  for the important class of processes controlled by the Edwards-Wilkinson equation.

We consider the average sign of the interfacial height stochastic variable measured at a fixed time  $t$  with respect to the original value corresponding to the initial position  $x_0$ ,

$$S_{av}(x) = \frac{1}{x} \int_0^x \text{sgn}[h(x_0 + x', t) - h(x_0, t)] dx'. \quad (2)$$

The spatial persistent large deviations probability is defined, in analogy with its temporal correspondent, as the probability that the average sign  $S_{av}$  remains persistently above a particular value  $s$ , with  $-1 \leq s \leq 1$ , up to a longer distance  $x$  measured from the initial position  $x_0$ ,

$$P_x(x, s) \equiv \text{Prob} \{S_{av}(x') \geq s, \forall x' \leq x\}. \quad (3)$$

We provide numerical evidence showing that  $P_x(x, s)$  has a power-law behavior for  $x < L$ , where  $L$  is the typical length scale in the numerical simulations (i.e., system size), independent of the choice of the average sign parameter  $s$ ,

$$P_x(x, s) \propto x^{-\theta_x(s)}, \quad (4)$$

where the spatial persistent large deviations exponent  $\theta_x(s)$  depends continuously on the parameter  $s$  that appears in the definition of the probability. The importance of  $P_x(x, s)$  lies in the fact that it provides an *infinite* family of persistence exponents, instead of only one exponent as in the case of  $P_x(x)$ . Obviously,  $P_x(x, s=1)$  and its associated exponent  $\theta_x(s=1)$  are precisely the spatial persistence probability and the nontrivial persistence exponent ( $\theta_{SS}$  or  $\theta_{FIC}$ , depending on the sampling procedure applied to  $x_0$ ), respectively. The opposite limit  $s \rightarrow -1$  is trivial in the sense that  $P_x(x, s=-1)=1$  independent of  $x$  and as a consequence  $\theta_x(s=-1)=0$ .

The  $s$  dependence of the temporal persistent large deviations exponents is known exactly for the simple random walk case, which is one of the few analytically solved persistence problems [18],

$$\theta_l(s) = \frac{2\theta_l(1)}{\pi} \arctan \sqrt{\frac{1+s}{1-s}}. \quad (5)$$

The mapping [15] between the *temporal* properties of the random walker (RW) problem and the *spatial* properties of the Edwards-Wilkinson (EW) fluctuating interfaces implies that the expression of Eq. (5) also applies to the distribution of the *spatial* persistent large deviations exponent as a function of  $s$ . This conjecture is verified numerically in this study.

In this paper, we have carried out the first application of the spatial persistent large deviations concept to the case of (1+1)-dimensional fluctuating interfaces characterized by the EW dynamical equation. Using the configuration of the interface corresponding to a fixed time of the order of the time required by the interface width to saturate (i.e.,  $t \sim L^z$ ), we have computed  $P_x(x, s)$  as the fraction of lattice sites  $x_j$  (with  $j=1, 2, \dots, L-1$ ) which maintained their stochastic variable  $S_{av}$  persistently above a fixed  $s$  value, up to a distance  $x_j+x$ . The initial measurement points,  $x_j$ , are sampled from the entire set of the steady-state interfacial profile. The numerical integration of the stochastic equation is performed using the simple forward-time centered-space representation [19]. We have used numerical systems of size  $L \sim 1000$  and we have averaged the results over many ( $\sim 1000$ ) independent runs to obtain convergent statistics.

In Fig. 1, we show the results for  $P_x(x, s)$  as a function of  $x$  for (1+1)-dimensional EW interfaces simulated numerically. We display ten log-log spatial persistent large deviations curves versus the distance  $x$  for ten values of the average sign parameter  $s$  (i.e.,  $s = +1, +0.8, \dots, -0.8$ ). We observe that  $P_x(x, s) \sim x^{-\theta_x(s)}$  for  $x < L/2$ , while for larger values of  $x$  and  $s \geq 0$  there is a downward deviation of the probability from the power-law behavior due to finite-size limitations. Except for the curve corresponding to  $s=1$ , which gives the usual spatial persistence exponent  $\theta_{SS}$

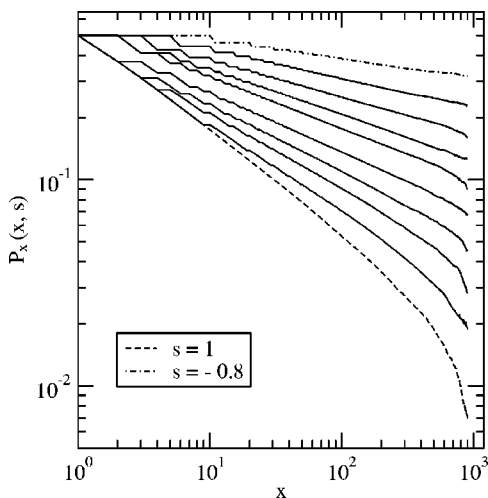


FIG. 1. Log-log plot of  $P(x,s)$  vs  $x$  for the EW equation based on the direct numerical integration of Eq. (1) with  $z=2$ , using a system of size  $L=1000$ . The average sign parameter takes ten different values decreasing from  $s=1$  (bottom curve) to  $s=-0.8$  (top curve) with an average sign difference  $\Delta s=0.2$ . All spatial persistent large deviations probabilities show power-law decay vs distance for  $x < L/2$ . The finite-size effects are responsible for the deviations of the probabilities from the power-law trend at large values of  $x$ .

$\approx 0.50$ , in agreement with Refs. [15,16], all the other curves with  $s < 1$  provide information concerning spatial behavior of the interface fluctuations.

The temporal persistent large deviations probability of the random walk model is shown in Fig. 2. We have used similar  $s$  values, as in the case of  $P_x(x,s)$  described above.  $P_t(t,s)$  shows a clear power-law behavior versus  $t$ . We find that  $P_t(t,s=1)$  is characterized by an exponent of 0.50, in agreement with the theoretical value  $\theta_t=1/2$ . Individual temporal

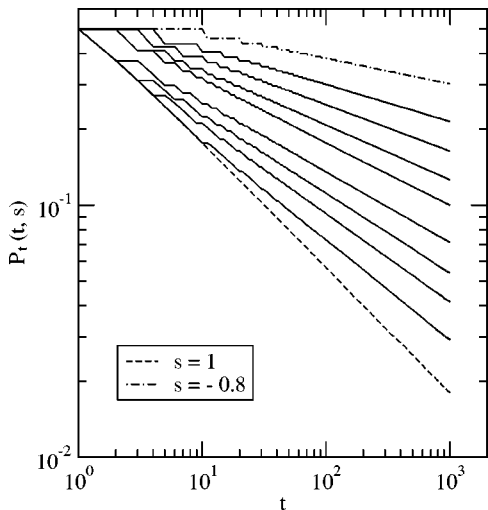


FIG. 2. Log-log plot of simulated  $P_t(t,s)$  vs  $t$  for the RW problem. The system size is  $L=500$  and the average sign parameter takes ten different values decreasing from  $s=1$  (bottom curve) to  $s=-0.8$  (top curve) with  $\Delta s=0.2$  between successive probability curves. All temporal persistent large deviations probabilities show power-law behavior vs time.

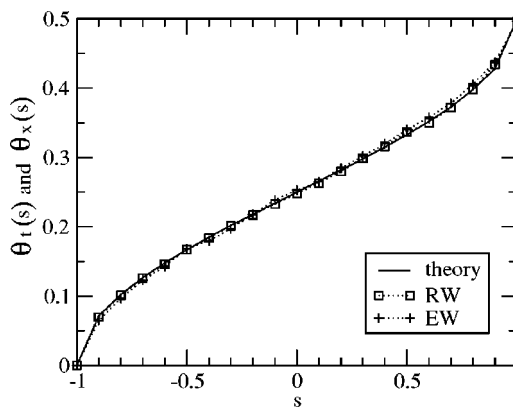


FIG. 3.  $\theta_t(s)$  and  $\theta_x(s)$  vs  $s$  as extracted from the power-law decay of  $P_t(t,s)$  (for the RW problem) and  $P(x,s)$  (for the EW fluctuating interfaces), respectively. The increment of the average sign parameter is  $\Delta s=0.1$ . The continuous curve represents the theoretical prediction of Eq. (5).

persistent large deviations exponents  $\theta_t(s)$  are extracted from the linear regions of the log-log plots of  $P_t(t,s)$  versus  $t$  and they are compared in Fig. 3 to the corresponding spatial set of exponents  $\theta_x(s)$  for the EW interfaces.

The level of agreement between  $P_x(x,s)$  corresponding to the EW dynamical equation and  $P_t(t,s)$  of the RW case can be seen in Fig. 3. To generate this figure we have used an increment of the average sign parameter ( $s$ ) of 0.1. We observe that the two sets of exponents,  $\theta_t(s)$  and  $\theta_x(s)$ , overlap very well within the errors of our simulations, showing that the mapping procedure involved in this study is perfectly applicable. Both cases are in agreement with the theoretical prediction of Eq. (5). We have also simulated a discrete stochastic growth model, the so-called Family model, which is theoretically known to exactly belong to the EW universality class [11]. The Family model results (not shown here) for  $P_x(x,s)$  and  $\theta_x(s)$  are very similar to those shown in Fig. 1 since they have identical stochastic dynamics.

Despite the downward deviation of the probability  $P_x(x,s)$  from the power-law behavior due to finite-size limitations, we have checked that larger system sizes would provide a wider range of distances over which the spatial persistence large deviations exponent can be extracted with a better precision. This can be seen in Fig. 4.

Another case of interest for epitaxial surface dynamics is growth under surface diffusion minimizing the local curvature, which belongs asymptotically to the Mullins-Herring (MH) [21] universality class [i.e., Eq. (1) with  $z=4$ ]. The exact mapping prediction by Majumdar and Bray [15] suggests that the spatial persistence properties of the continuum version of the growth models belonging to this universality class could be mapped onto the temporal persistence characteristics of the random acceleration problem described by the stochastic random equation  $d^2x/dt^2 = \eta(t)$  with an analytically known exponent of  $\theta_t=1/4$  [20]. One expects to obtain  $\theta_{SS}=0$  and  $\theta_{FIC}=1/4$  [15] when measuring the steady-state and finite initial conditions regimes of  $P_x(x)$ , respectively, for the Mullins-Herring surface growth dynamics. An example of this case is the (1+1)-dimensional model introduced by

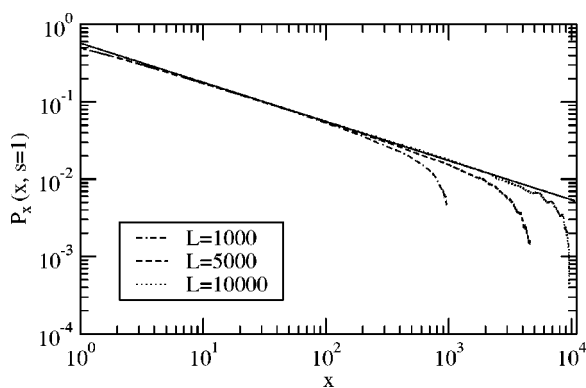


FIG. 4. Log-log plot of  $P_x(x, s)$  for  $s=1$  corresponding to the EW equation based on the direct numerical integration of Eq. (1) with  $z=2$ , using three system sizes, as shown in the legend. The straight line represents the fit for  $L=10^4$  simulation, providing an exponent of  $1/2$ .

Kim and Das Sarma [22]. This discrete solid-on-solid atomistic model, the so-called larger curvature (LC) model [22], is known to belong asymptotically to the MH universality class. As a consequence, we focus on the measurement of  $P_{\text{FIC}}(x)$  for the discrete LC model [22], since  $P_{\text{SS}}(x)$  is trivially described by a null exponent. The definition of  $P_{\text{FIC}}(x)$  involves the selection of the subset of sites characterized by *finite* height and height derivatives. One possibility would be to sample over the subset of sites placed on the average level. However, it turns out that a system with  $L=200$ , which is the typical system size in our simulations, usually has only a couple of discrete positions on the average level. For this reason, we have sampled over all the lattice sites  $x_j$  with the height variable (measured with respect to the average level) within a band of values characterized by a width  $w$  [i.e.,  $-w/2 \leq h(x_j) \leq w/2$ ], where  $w$  is taken to be smaller than the maximum magnitude of interface fluctuations. This selection ensured the possibility of sampling over a reasonable number of lattice sites presumably sufficient for good statistical results of  $P_{\text{FIC}}(x)$ .

In Fig. 5, we show the  $x$  dependence of  $P_{\text{FIC}}(x)$  corresponding to the LC discrete model for three values of  $w$ : 30, 70, and 110, respectively. The steady-state probability is shown for comparison. We note that  $P_{\text{FIC}}(x)$  does not display the expected power-law behavior as a function of  $x$ . As the bandwidth  $w$  increases, more and more lattice sites are included in the sampling subset, and  $P_{\text{FIC}}(x)$  tends to reach the behavior displayed by  $P_{\text{SS}}(x)$ . In addition, we observe that when using a numerical system with  $L=200$ ,  $P_{\text{SS}}(x)$  has a rather linear dependence on  $x$ , for  $50 < x < 200$ . The impossibility to recover the theoretically predicted behavior of  $P_{\text{FIC}}(x)$  may be due to the reduced system size used in our simulations. This limitation is imposed by the requirement of measuring the probability  $P_{\text{FIC}}(x)$  using an ensemble of steady-state configurations that can be achieved only by using an extensive computational time  $\sim L^4$ . We note that reducing or increasing the system size by a factor of 2 did not produce any qualitative change in the overall behavior of  $P_{\text{FIC}}(x)$  or  $P_{\text{SS}}(x)$ . In addition, we have checked that the direct numerical integration of Eq. (1) with  $z=4$  provides re-

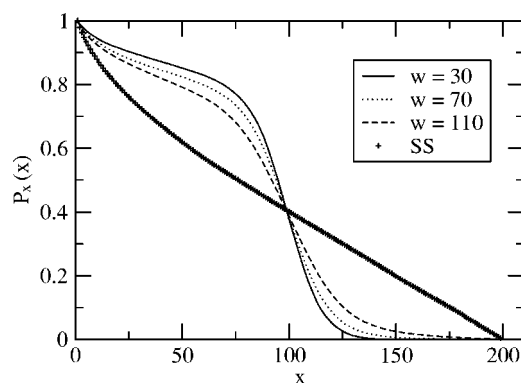


FIG. 5. Numerical results of  $P_{\text{FIC}}(x)$  and  $P_{\text{SS}}(x)$  for the LC discrete model with system size  $L=200$ . The measurements are performed from steady-state configurations.  $P_{\text{FIC}}(x)$  probabilities have been obtained by using three different band widths, as shown in the legend.  $P_{\text{FIC}}(x)$  does not display a power-law behavior as a function of  $x$  over the entire range of system size.

sults consistent with the discrete LC model. Also, it turns out that similar probability curves are obtained for solid-on-solid models belonging asymptotically to the molecular beam epitaxy universality class [such as the (1+1)-dimensional DT model [23]]. We believe that our problem with the spatial persistence  $P_x(x)$  for the LC model belonging to the MH universality class [22] arises most likely from the severe finite-size problems in simulating systems with large values ( $z=4$ ) of the dynamical exponent. Large dynamical exponent implies very slow lateral correlations, which considerably complicates studying steady-state behavior in the MH universality problem. In fact, this issue is very well known in traditional studies of dynamical scaling involving surface phenomena characterized by a large value of the dynamical exponent [24]. A large variety of stochastic discrete models show long-time transients and they cross over very slowly to their corresponding asymptotic behavior. Only extensive simulations of stochastic discrete models in the MH universality class can provide the asymptotic dynamical scaling associated with the continuous limit of Eq. (1) with  $z=4$ . This forbids us from pursuing further measurements of  $P_x(x, s)$  for the MH universality class and checking the validity of the mapping procedure, which remains an interesting open problem.

To conclude, we have shown numerically that the spatial persistent large deviations probability represents a possible generalization of the spatial persistence probability, providing a useful family of spatial exponents for the surface growth phenomena. We have mapped these exponents into the family of temporal persistent large deviations exponents obtained from the evolution of a simple stochastic “random walk” process. We have established the validity of this generalization for the case of fluctuating interfaces described by the Edwards-Wilkinson evolution equation. However, the similar problem involving the Mullins-Herring universality class remains open since the corresponding discrete LC model [22] simulation shows severe finite-size problems.

This work is partially supported by NSF-DMR-MRSEC and U.S. ONR.

- [1] C. W. Gardiner, *Handbook of Stochastic Methods for Physics, Chemistry and the Natural Sciences* (Springer-Verlag, Berlin, 1983).
- [2] J. Grasman, *Asymptotic Methods for the Fokker-Planck Equation and the Exit Problem in Applications* (Springer-Verlag, Berlin, 1999).
- [3] M. Marcos-Martin, D. Beysens, J. P. Bouchaud, C. Godreche, and I. Yekutieli, *Physica A* **214**, 396 (1995); W. Y. Tam, R. Zeitak, K. Y. Szeto, and J. Stavans, *Phys. Rev. Lett.* **78**, 1588 (1997); B. Yurke, A. N. Pargellis, S. N. Majumdar, and C. Sire, *Phys. Rev. E* **56**, R40 (1997); G. P. Wong, R. W. Mair, R. L. Walsworth, and D. G. Cory, *Phys. Rev. Lett.* **86**, 4156 (2001).
- [4] D. B. Dougherty, I. Lyubinetzky, E. D. Williams, M. Constantin, C. Dasgupta, and S. Das Sarma, *Phys. Rev. Lett.* **89**, 136102 (2002).
- [5] D. B. Dougherty, O. Bondarchuk, M. Degawa, and E. D. Williams, *Surf. Sci.* **527**, L213 (2003).
- [6] J. Merikoski, J. Maunuksela, M. Myllys, J. Timonen, and M. J. Alava, *Phys. Rev. Lett.* **90**, 024501 (2003).
- [7] For a review, see S. N. Majumdar, *Curr. Sci.* **77**, 370 (1999); J. Krug, e-print cond-mat/0403267.
- [8] A.-L. Barabasi and H. E. Stanley, *Fractal Concepts in Surface Growth* (Cambridge University Press, New York, 1995).
- [9] H. Jeong and E. D. Williams, *Surf. Sci. Rep.* **34**, 171 (1999).
- [10] J. Krug, H. Kallabis, S. N. Majumdar, S. J. Cornell, A. J. Bray, and C. Sire, *Phys. Rev. E* **56**, 2702 (1997).
- [11] M. Constantin, C. Dasgupta, P. Punyindu Chatraphorn, S. N. Majumdar, and S. Das Sarma, *Phys. Rev. E* **69**, 061608 (2004).
- [12] I. Dornic and C. Godreche, *J. Phys. A* **31**, 5413 (1998).
- [13] T. J. Newman and Z. Toroczkai, *Phys. Rev. E* **58**, R2685 (1998); Z. Toroczkai, T. J. Newman, and S. Das Sarma, *ibid.* **60**, R1115 (1998).
- [14] M. Constantin, S. Das Sarma, C. Dasgupta, O. Bondarchuk, D. B. Dougherty, and E. D. Williams, *Phys. Rev. Lett.* **91**, 086103 (2003).
- [15] S. N. Majumdar and A. J. Bray, *Phys. Rev. Lett.* **86**, 3700 (2001).
- [16] M. Constantin, S. Das Sarma, and C. Dasgupta, *Phys. Rev. E* **69**, 051603 (2004).
- [17] S. F. Edwards and D. R. Wilkinson, *Proc. R. Soc. London, Ser. A* **381**, 17 (1982).
- [18] A. Baldassarri, J. P. Bouchaud, I. Dornic, and C. Godreche, *Phys. Rev. E* **59**, R20 (1999).
- [19] W. H. Press *et al.*, *Numerical Recipes* (Cambridge University Press, Cambridge, 1989).
- [20] T. W. Burkhardt, *J. Phys. A* **26**, L1157 (1993); Y. G. Sinai, *Theor. Math. Phys.* **90**, 219 (1992).
- [21] W. W. Mullins, *J. Appl. Phys.* **28**, 333 (1957); C. Herring, *ibid.* **21**, 301 (1950).
- [22] J. M. Kim and S. Das Sarma, *Phys. Rev. Lett.* **72**, 2903 (1994); J. Krug, *ibid.* **72**, 2907 (1994).
- [23] S. Das Sarma and P. Tamborenea, *Phys. Rev. Lett.* **66**, 325 (1991).
- [24] S. Das Sarma, C. J. Lanczycki, R. Kotlyar, and S. V. Ghaisas, *Phys. Rev. E* **53**, 359 (1996); P. Punyindu and S. Das Sarma, *ibid.* **57**, R4863 (1998).